Continuous wave electron paramagnetic resonance investigation of the hyperfine structure of 17 O 2 adsorbed on the MgO surface

Mario Chiesa, Elio Giamello, M. Cristina Paganini, Zbigniew Sojka, and Damien M. Murphy

Citation: The Journal of Chemical Physics **116**, 4266 (2002); doi: 10.1063/1.1447907
View online: http://dx.doi.org/10.1063/1.1447907
View Table of Contents: http://scitation.aip.org/content/aip/journal/jcp/116/10?ver=pdfcov
Published by the AIP Publishing

Continuous wave electron paramagnetic resonance investigation of the hyperfine structure of $^{17}O_2^-$ adsorbed on the MgO surface

Mario Chiesa, Elio Giamello,[a),b)] and M. Cristina Paganini
Dipartimento di Chimica IFM, Università di Torino, e Unità INFM di Torino, Via Giuria, 7-10125 Torino, Italy

Zbigniew Sojka[a),c)]
Department of Chemistry, Jagiellonian University, ul. Ingardena 3, 30-060 Cracow, Poland

Damien M. Murphy
Department of Chemistry, Cardiff University, P.O. Box 912, Cardiff CF10 3TB, United Kingdom

(Received 10 September 2001; accepted 11 December 2001)

The adsorption of molecular oxygen (enriched with ^{17}O) onto high surface area MgO has been studied by electron paramagnetic resonance (EPR) spectroscopy. The oxide surface was pretreated in such a way so that surface trapped electron $F_S^+(H)$ centers are produced. Subsequent dioxygen adsorption results in an electron transfer reaction from $F_S^+(H)$ centers to O_2, producing a surface stabilized superoxide (O_2^-) anion. The resulting EPR spectrum of the paramagnetic anion is complicated by the simultaneous presence of a high number of ''normal'' hyperfine lines along the principal axes and also by several off-axis extra features which have complicated previous interpretations of the A_{yy} and A_{zz} components. By adopting a suitable adsorption procedure which suppresses the superoxide speciation, using a highly crystalline MgO material and controlling the isotopomer composition through appropriate ^{17}O enrichments, the resolution of the EPR spectrum has been dramatically improved. Analysis of the ^1H superhyperfine structure ($|\mathbf{A}^H|/\beta_e g = [3.9,2.2,1.3]G$), resulting from a dipolar interaction between the adsorbed O_2^- anion and a neighboring OH group, and positions of the extra absorption lines in the spectrum, have provided us with auxiliary sources of information to determine for the first time the complete ^{17}O hyperfine tensor ($\mathbf{A}^O/\beta_e g = [-76.36,7.18,8.24]$ G). The tensor has been analyzed in detail using a localized spin model. The spin density is shared among the $2p_\pi^x(0.495)$, $2p_x^y(-0.024)$ and $2s(0.011)$ orbitals. The total spin density on O_2^- indicates that a complete surface electron transfer from the $F_S^+(H)$ center to dioxygen occurs upon adsorption, in line with recent *ab initio* calculations.
 [DOI: 10.1063/1.1447907]

I. INTRODUCTION

The chemistry of oxygen species at solid surfaces has attracted the attention of several research groups over the years due to its relevance in various fields of modern science such as heterogeneous catalysis, material science, electrochemistry and corrosion. Owing to its peculiar properties, related to the $^3\Sigma_g^-$ ground state that hinders the reactivity, dioxygen is usually activated on catalytic surfaces by a gradual reduction process: $O_{2(g)} \rightarrow O_{2(a)} \rightarrow O_{2(a)}^- \rightarrow O_{(a)}^- \rightarrow O_{2(a)}^{2-} \rightarrow O_{(L)}^{2-}$. Many experimental and theoretical investigations have been devoted to this activation process, starting from the early stages of O_2^- formation until final incorporation of the resultant O^{2-} ion into the oxide lattice.[1] In particular, the EPR technique has singularly advanced our understanding of the nature of the paramagnetic oxygen intermediates appearing along this pathway, and also helped to characterize their molecular structure.[2–4]

The surface adsorbed superoxide anion is usually identified on the basis of its **g** tensor. However, the initial unambiguous proof for its formation and stabilization at a surface was obtained by analysis of the hyperfine pattern from the spectra obtained with ^{17}O-enriched molecular oxygen. The natural abundance of this isotope, having a nuclear spin of $\frac{5}{2}$, is very low (0.038%) and the EPR spectra are dominated by the structureless signal due to the more abundant ^{16}O and ^{18}O isotopes with $I=0$ (99.7%).

In a pioneering paper by Tench and Holroyd,[5] the ^{17}O hyperfine structure of the superoxide anion adsorbed on polycrystalline MgO was first reported. The authors used molecular oxygen with an isotopic enrichment of 58%. The EPR powder spectrum was, however, quite complicated due to the simultaneous presence of hyperfine patterns arising from both $(^{17}O–^{16}O)^-$ and $(^{17}O–^{17}O)^-$ superoxide species superimposed on the structureless signal of the $(^{16}O–^{16}O)^-$ isotopomer. Furthermore, the simultaneous presence of several distinct O_2^- species on the polycrystalline surface (O_2^- speciation) added more complications to the EPR spectrum. Since the symmetry of the A^O tensor for the adsorbed superoxide is orthorhombic, the number of expected hyperfine lines is large and in the spectrum reported by Tench and Holroyd,[5] only the largest component (A_{xx}) had a clearly

a)Authors to whom correspondence should be addressed.
b)Electronic mail: elio.giamello@unito.it
c)Electronic mail: sojka@chemia.uj.edu.pl

resolved structure. This was sufficient, however, to enable the authors[5] to unambiguously establish the diatomic nature of the adsorbed species and demonstrate the magnetic equivalence of the two oxygen atoms. This latter observation indicates a ''side-on'' bonding of the superoxide species. The resolution of the EPR spectrum was, however, insufficient for a reliable assignment of the remaining components (A_{yy} and A_{zz}) of the hyperfine tensor, and the reported estimates ($A_{yy}=0$ G and $A_{zz}=15$ G)[5] have never been verified by simulation of the spectrum. As a result, until now the complete ^{17}O hyperfine tensor of the surface O_2^- radical remains still unknown.

The complete resolution of the hyperfine structure is necessary in order to understand another crucial factor related to the structure of the superoxide anion on MgO, i.e., the distribution of the electron spin density on the adsorbed species. This is important from the viewpoint of the surface chemistry, since as discussed by Tench and Holroyd,[5] the anion is generated by electron transfer from surface point defects containing a single trapped electron [the $F_S^+(H)$ center]. In this case the total spin density on O_2^- reflects the degree of electron transfer from the defect to the adsorbed molecule. The magnetic properties of these $F_S^+(H)$ color centers, and their subsequent electron transfer reactions with various adsorbed molecules, have been the subject of several recent investigations.[6–11] In particular, it has been demonstrated that adsorbed N_2^- radical anions are generated and stabilized on the MgO surface by the reaction of dinitrogen with $F_S^+(H)$ centers at 77 K.[12,13] The remarkable resolution of the N_2^- spectrum was achieved, in part, by the use of a highly crystalline MgO sample with high surface area ($\approx$300 $m^2\,g^{-1}$), produced by a chemical vapor deposition (CVD) technique. The high resolution of the N_2^- spectra obtained with this CVD MgO material prompted us to revisit the EPR spectrum of the adsorbed $^{17}O_2^-$ anion on the same material.

The present article provides results of the simulation and in depth analysis of the complex EPR spectra obtained when dioxygen enriched in ^{17}O at two different levels is adsorbed on CVD MgO containing surface $F_S^+(H)$ centers. The methodology adopted for the interpretation of the resultant powder spectrum consists in the simplification of the system by suppressing O_2^- speciation, by control of the isotopomer composition and, finally, by utilization of the superhyperfine and extra absorption lines in order to determine the complete ^{17}O hyperfine tensor.

II. EXPERIMENT

All experiments were carried out with polycrystalline magnesium oxide prepared by a chemical vapor deposition method[14] and kindly supplied by Professor E. Knözinger (Technische Universitat, Wien). The MgO powder, with a surface area of $\approx$300 m^2/g, was thermally activated at 1173 K for 1 h under a dynamic vacuum (10^{-5} Torr). The $F_S^+(H)$ or $F_S^+(D)$ color centers were generated on the surface of the activated oxide as described in detail elsewhere.[6–11] Briefly, hydrogen or deuterium ($\sim$100 Torr, 1 Torr=133 Pa) was added to the activated oxide at 298 K and the powder was subsequently cooled to 77 K. The sample was then irradiated using a low pressure UV mercury vapor lamp for about 1 h. The excess H_2 or D_2 was then slowly evacuated at 298 K from the pale blue colored sample. The colored sample exhibits an EPR spectrum characterized by a hyperfine doublet due to the interaction of the electron with the proton of a neighboring OH group. The hyperfine pattern is unresolved for the $F_S^+(D)$ center, since activation in D_2 leads to the formation of surface OD groups. The superoxide radical anion was generated by exposure of the sample to oxygen (0.5 Torr). Two different ^{17}O isotopic enrichment, 28% and 63%, were used. All isotopic gases were supplied by ICON SERVICE Inc. (New Jersey, USA) and used without further purification. The relative abundance P^{nm} of the isotopomers ($^{16}O_2$, $^{17}O^{16}O$, and $^{17}O_2$) present in the gas mixture is given by $P^{16\text{-}16}=(1-p)^2$, $P^{16\text{-}17}=2p(1-p)$, and $P^{17\text{-}17}=p^2$, where p is the ^{17}O enrichment level. The number of lines and the abundance of the oxygen isotopomers are summarized in the following scheme for the two isotropic enrichments used in this study:

Species	^{16}O-^{16}O	^{16}O-^{17}O ^{16}O-^{17}O	^{17}O-^{17}O
Concentration	$(1-x)^2$	$2x\,(1-x)$	x^2
n° of lines	1	6	11

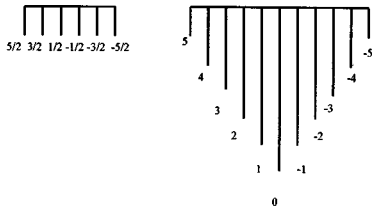

The EPR spectra were recorded at 77 K on a Bruker EMX spectrometer operating at *X*-band frequencies. Simulations were carried out using a program (developed by Mabbs and Collison[15]) which calculates exact solutions for the spin Hamiltonian by performing matrix diagonalization.

III. EPR SPECTRUM OF THE $^{17}O_2^-$ SURFACE SPECIES

The two principal modes of superoxide adsorption correspond to a ''side-on'' η^2 structure with equivalent nuclei and a ''top-on'' η^1 structure with nonequivalent nuclei. As shown by Tench and Che, they can be readily distinguished using ^{17}O labeled oxygen.[2,3] The case of MgO, where O_2^- radicals are stabilized at the surface with both oxygens magnetically equivalent, and the case of Mo/SiO_2, where they are distinctly nonequivalent, may serve here as good examples.[5,16,17]

The free superoxide radical exhibits a $\sigma_g^4\pi_u^4\pi_g^3$ electronic configuration and the $^2\Pi_{3/2}$ ground state. The corresponding magnetic moment due to orbital and spin angular momentum is proportional to $\Lambda+g_e\Sigma=\pm 2$ and causes the **g** tensor to be extremely anisotropic with $g_\parallel=2\langle+1,+\frac{1}{2}|L_z+2S_z|+1,+\frac{1}{2}\rangle=4$, and $g_\perp=\langle+1,-\frac{1}{2}|L_x+2S_x|-1,+\frac{1}{2}\rangle=0$. As a result the powder spectrum of the superoxide radi-

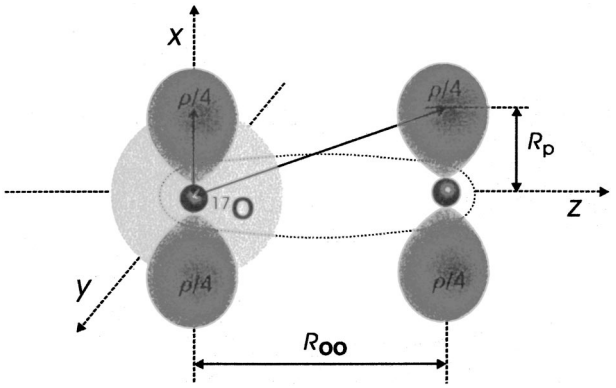

FIG. 1. Schematic illustration of the principal directions (X,Y,Z) for the superoxide (O_2^-) radical anion. See text for description of other terms.

cal will extend over a large magnetic field and consequently will be too weak to be detected, unless the orbital momentum is partially quenched by the strong interaction with the environment,[18] as occurs for trapped or adsorbed state.

The trapped rigid species enriched in ^{17}O $(I=\frac{5}{2})$ with equivalent nuclei usually exhibits an orthorhombic EPR spectrum that is accounted for by the following spin Hamiltonian:

$$\mathbf{H}=\mu_B\mathbf{B}^T\cdot\mathbf{g}\cdot\mathbf{S}+\mathbf{S}^T\cdot\mathbf{A}\cdot\mathbf{I}+\mathbf{I}^T\cdot\mathbf{P}\cdot\mathbf{I} \tag{1}$$

with $g_z \gg g_y > g_x$ and $A_x \gg A_y, A_x$. The z direction is defined as along the internuclear axis, while x and y directions corresponds to the in-plane and out-of-plane $2p_\pi$-orbitals, respectively (Fig. 1). Due to the relatively small value of the quadrupole moment of the ^{17}O nuclei $(Q_O=-0.026)$, the quadrupole effects $(\mathbf{I}^T\cdot\mathbf{P}\cdot\mathbf{I})$ do not influence the powder pattern to an appreciable extent[19] and can be neglected. In the case of the doubly labeled $(^{17}O–^{17}O)^-$ species, it is useful to define a total nuclear spin number $I=I_1+I_2(\frac{5}{2}+\frac{5}{2}=5)$ as a convenient label for the hyperfine transitions. The simulation of the spectrum has been carried out by adding the signals of the three isotopomers $(^{16}O–^{16}O)^-$, $(^{17}O–^{16}O)^-$, and $(^{17}O–^{17}O)^-$ using the same **g** and **A** tensors, but weighted by their relative abundance in the gas mixture.

In a randomly oriented sample the number of features in the EPR spectrum is determined by the following condition:[20]

$$\partial B/\partial\theta=0 \quad \text{and} \quad \partial B/\partial\phi=0. \tag{2}$$

The three solutions, where $\theta=0(B_z)$, $\theta=\pi|2$, and $\phi=0(B_x)$, $\theta=\pi/2$ and $\phi=\pi/2(B_y)$, correspond to the usual principal components. For each principal direction of the **g** tensor the signal is additionally split into $2I+1=6$ lines in the case of $^{16}O^{17}O^-$ isotopomer and into $2nI+1=11$ lines for $^{17}O^{17}O^-$ species with even nuclei. Because the nuclear magnetic moment of ^{17}O is negative $(g_O=-0.757\,52)$, the successive hyperfine satellites appearing with increasing magnetic field are transitions from $m_1=\frac{5}{2}$ to $m_1=-\frac{5}{2}$, for singly labeled species, and from $m_1=5$ to $m_1=-5$ for doubly labeled species, respectively.[21] The intensity of these lines and their detectability depends essentially on the degree of the oxygen enrichment. At low enrichment levels (20%–30%), the signal due to the singly labeled molecules is dominant (scheme 1), while for mixtures containing 60–70% of ^{17}O the patterns from both singly and doubly labeled superoxide radicals can be simultaneously observed, producing up to 51 lines in the EPR spectrum.

However, this relatively simple situation becomes more complicated due to the additional effect of a large anisotropy in the ^{17}O hyperfine tensor and a high nuclear spin quantum number. This favors the appearance of extra lines in the powder spectrum, when the following inequalities are satisfied:

$$2A_i^2-h\upsilon A_i/m<(g_i^2A_i^2-g_j^2A_j^2)/(g_i^2-g_j^2) \\ <2A_j^2-h\upsilon A_j/m, \tag{3}$$

where υ is the microwave frequency, and m is the nuclear magnetic spin number. These extra features, also known as "overshoots," correspond to additional solutions $(\partial B/\partial\theta=0$ and $\partial B/\partial\phi=0)$ in the ij plane, and therefore do not coincide with the principal magnetic components.[22] The appearance of extra lines, which can exhibit significant intensity, may be used to determine some less resolved components of the experimental spectrum (*vide infra*).

IV. RESULTS AND INTERPRETATION

A. EPR spectra and determination of the spin Hamiltonian parameters

The adsorbed O_2^- anion was generated on the MgO sample by bleaching the $F_S^+(H)$ color centers with a small amount of O_2 (<0.5 Torr) at liquid nitrogen temperature. Assuming local C_{2v} symmetry for the adsorbed O_2 (Ref. 23) we may write

$$F_S^+(^2A_1)+O_{2(g)}(^3\Sigma_g^-)\rightarrow F_S^{2+}-O_{2(ads)}^-(^2B_1). \tag{4}$$

At this reaction temperature, the O_2^- species dominate at a single surface site (i.e., one does not observe the simultaneous presence of several groups of O_2^- radicals with different g_z caused by surface heterogeneity), so that a well resolved superoxide EPR spectrum of $^{16}O_2^-$ is obtained [Fig. 2(a)]. This spectrum is characterized by $g_{zz}=2.0770$, $g_{yy}=2.0083$, and $g_{xx}=2.0016$. Closer inspection of the spectrum reveals that the O_2^- spectral lines are actually split by a superhyperfine interaction between the O_2^- anion and a proton from the nearby OH group.[24] This interaction can be fully resolved $(|A_{xx}^H|=3.9$ G, $|A_{yy}^H|=2.2$ G, $|A_{zz}^H|=1.3$ G) and the ^1H splitting can be rationalized in terms of a through space dipolar interaction as discussed in detail elsewhere.[25] Since the $O_2\cdots H$ complex possesses a C_s symmetry, the principal axes of the **g** and $\mathbf{A}^H$ tensors are not necessarily coincident, and the observed values may not correspond to the principal components of the proton superhyperfine interaction. In the case of the $F_S^+(D)$ centers, by comparison, the weak superhyperfine splitting due to deuterium is too small, as it can be deduced from the corresponding $\mathbf{A}^H$ tensor $(|\mathbf{A}^D|=g_D/g_H|\mathbf{A}^H|=[0.6,0.3,0.2]$ G), and remains unresolved. All of the magnetic parameters are summarized in Table I.

The analysis of the ^{17}O-enriched superoxide spectra [Figs. 2(b) and 2(c)] is rather complex but has been appreciably simplified due to two favorable circumstances. In the

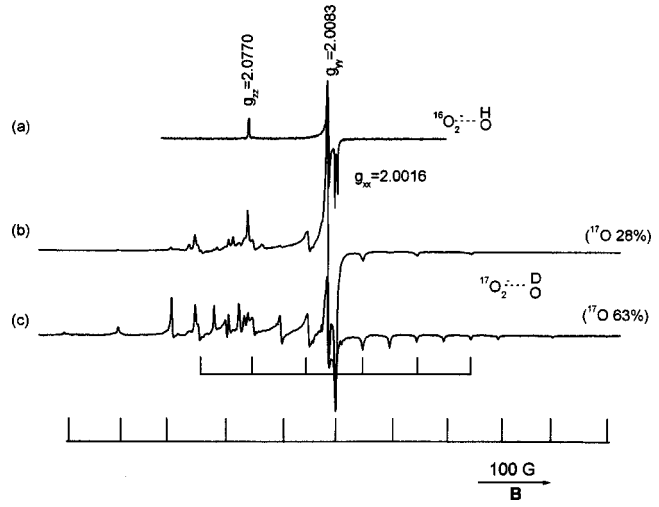

FIG. 2. EPR spectra (at 77 K) of (a) $^{16}O_2^-$, (b) O_2^- (28% ^{17}O enriched), and (c) O_2^- (63% ^{17}O enrichment), adsorbed on the MgO surface. The $^{16}O_2^-$ radical (a) was formed by reaction of $^{16}O_2$ with surface F_S^+(H) centers, while the ^{17}O enriched O_2^- radicals [(b) and (c)] were formed using F_S^+(D) centers.

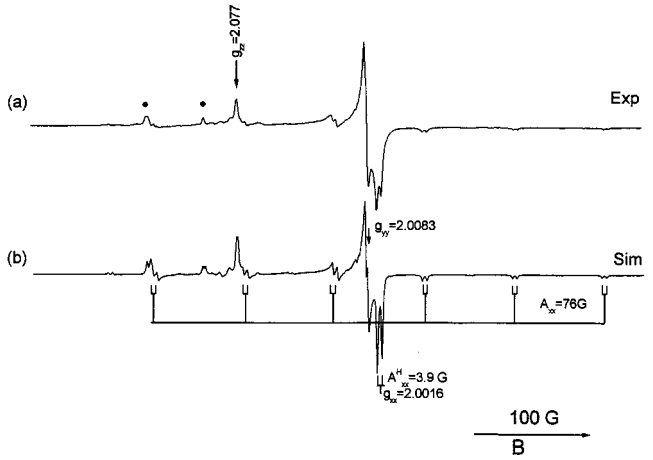

FIG. 3. Experimental (a) and computer simulated (b) EPR spectrum of the 28% ^{17}O enriched O_2^- radical on MgO. The A_{xx}^{O} and A_{xx}^{H} coupling are illustrated with the stick diagrams.

first case, a negligible speciation of surface O_2^- occurs, due to the low temperatures of adsorption. In the second case, a well resolved ^{1}H hyperfine coupling is manifested in every line of the ^{17}O hyperfine structure. As a result, comparison of the two types of ^{17}O hyperfine patterns (with and without a ^{1}H superhyperfine structure due to $O_2^-\cdots$H and $O_2^-\cdots$D interactions, respectively) provides useful guidelines for the full interpretation of the $^{17}O_2^-$ EPR spectrum.

The EPR spectra obtained by bleaching the F_S^+(D) centers with dioxygen containing 28% and 63% of ^{17}O are shown in Figs. 2(b) and 2(c), respectively. For the 28% enriched sample, the contribution of the doubly labeled $(^{17}O–^{17}O)^-$ species to the overall spectrum is small ($P^{17\text{-}17}=7\%$) and distributed over 11 lines, which remain practically undetectable. The resulting spectrum is therefore greatly simplified, and practically displays the $(^{17}O–^{16}O)^-$ hyperfine structure only. The largest splitting corresponds to $A_{xx}=76$ G, which is in agreement with previous reports.[5,16,26] However, in the case of the sample with 63% ^{17}O enrichment, the $(^{17}O–^{16}O)^-$ and $(^{17}O–^{17}O)^-$ hyperfine patterns appear simultaneously [see stick diagram in Fig. 2(c)]. The presence of a distinct 11-line pattern clearly indicates that both nuclei are magnetically equivalent, implying the formation of a "side-on" η^2 $O_2^-–Mg^{2+}$ electrostatic complex.

The EPR spectrum of O_2^- obtained by reacting the F_S^+(H) centers with 28% enriched ^{17}O is shown in Fig. 3 along with its computer simulation. Each line of the hyperfine sextet is split by 3.9 G along the x direction due to the interaction with the adjacent OH group. For clarity of presentation, the A_{xx}^{O} and A_{xx}^{H} lines are emphasized by the stick diagram on the simulated spectrum [Fig. 3(b)]. Two rather intense lines, marked with dots in Fig. 3(a), that are not accounted for by the A_{xx}^{O} pattern, have been identified as off-axis extra absorption lines. The nature of these extra lines is discussed below in more detail.

The relative clarity and resolution of the EPR spectrum in Fig. 3 permitted us to thoroughly analyze the hyperfine coupling constants in the y and z directions, so that a complete determination of the $\mathbf{A}^O$ tensor could be obtained. To illustrate this point, magnification of the g_{yy} region of this spectrum is shown in Fig. 4(a) along with the corresponding simulated fragment [Fig. 4(b)]. Six hyperfine lines centered at $g_{yy}=2.0083$ and separated by a 7.8 G can be clearly identified, as indicated by the stick diagram in Fig. 4(a). This assignment is strongly supported by the fact that each line is additionally split into a doublet of 2.2 G. This latter value corresponds exactly to the ^{1}H superhyperfine splitting of the g_{yy} component determined earlier from the $^{16}O_2^-$ spectrum [see Fig. 2(a) and Table I]. Thus, although the ^{17}O hyperfine lines are rather weak, the A_{yy}^{O} component could be determined quite reliably.

The analysis of the g_{zz} region is, by far, more demanding. The expanded fragment of this region, along with its simulation, is shown in Fig. 5. This portion of the spectrum is the most congested, due to the superimposition of the A_{zz}

TABLE I. Spin-Hamiltonian parameters for adsorbed $^{17}O_2^-$ radical ion on MgO.

	g tensor			^{17}O hyperfine tensor (G)				^{1}H superhyperfine tensor (G)		
	g_{xx}	g_{yy}	g_{zz}	$^{17}a_{iso}$	$^{17}B_{xx}$	$^{17}B_{yy}$	$^{17}B_{zz}$	$^{H}A_{xx}$	$^{H}A_{yy}$	$^{H}A_{zz}$
Experimental	2.0016	2.0083	2.0770	−20.3	−56.0	+27.5	+28.6	3.9	2.2	1.3
Calculated[a]				−9.67	−56.3	+27.7	+28.7			

[a]Values taken from Ref. 32.

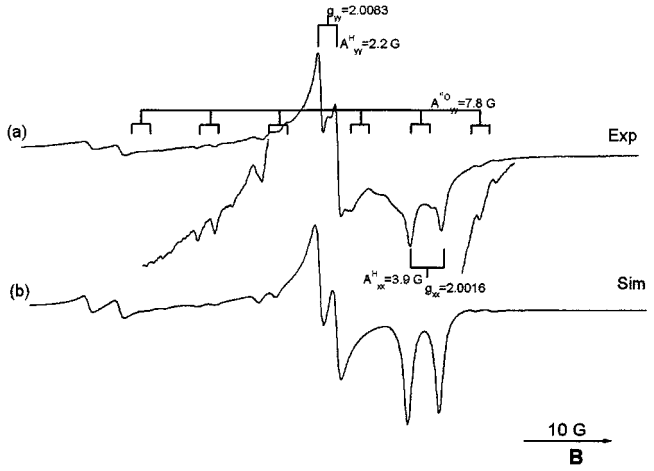

FIG. 4. Expanded part of the g_{xx}, g_{yy} region of the 28% ^{17}O enriched O_2^- (Fig. 3). (a) Experimental and (b) computer simulation.

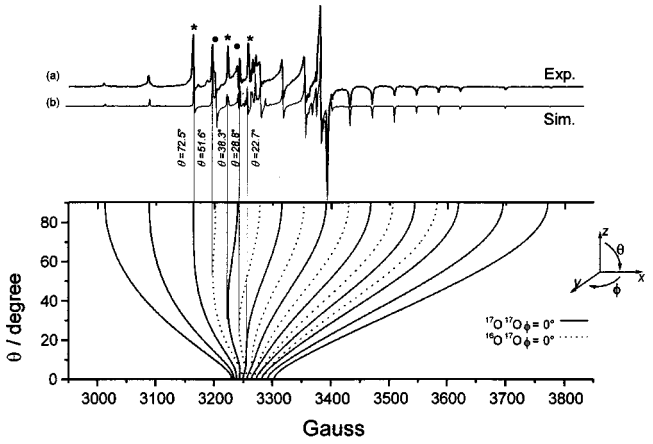

FIG. 6. (a) Experimental and (b) computer simulated EPR spectra of 63% ^{17}O enriched O_2^- generated by reaction with F_S^+(D) centers. The spectrum contains contribution from $(^{16}O–^{16}O)^-$, $(^{17}O–^{16}O)^-$, and $(^{17}O–^{17}O)^-$ species. The angular dependencies of the hyperfine lines are also shown. The positions of the off-axis "overshoot" features are indicated with the * (17-17 structure) and • (16-17 structure) symbols.

pattern of ^{17}O combined with the g_{zz} component of ^{16}O (i.e., the dominant single at $g_{zz}=2.0770$ with $|A^{H}|=1.3$ G) and the $m_1=\frac{3}{2}$ and $m_1=\frac{5}{2}$ lines due to the A_{xx} hyperfine structure. Further complications in the assignment are created due to the presence of two off-axis extra lines (marked with dots in Fig. 5) and the absence of a resolved ^1H superhyperfine splitting, which previously proved helpful in the interpretation of the g_x and g_y regions.

Nevertheless, although the six line A_{zz}^{O} hyperfine pattern is not very clearly resolved in the spectrum, the assignment can be corroborated by the independent evaluation of $|A_{zz}^{O}|$ through the analysis of the positions of the five extra lines (marked with dots and asterisks in Fig. 6) which were observed in the spectra of $(^{16}O–^{17}O)^-$ and $(^{17}O–^{17}O)^-$. In the latter case, a 63% ^{17}O enriched mixture was used to generate the $(^{17}O–^{17}O)^-$ species (Fig. 6). The assignment was further refined and improved by simulation and the best fit was obtained for a value of $|A_{zz}^{O}|=7.3$ G [Fig. 5(b)]. This value is two to three times smaller than previous reports of A_{zz} for O_2^- on MgO (15–20 G).[3] This rather large discrepancy is most likely due to the incorrect interpretation of the spectra in the past, particularly in the z/zx region, rather than originating from any significant differences in the electronic structure of the superoxide species observed in the different reported cases.

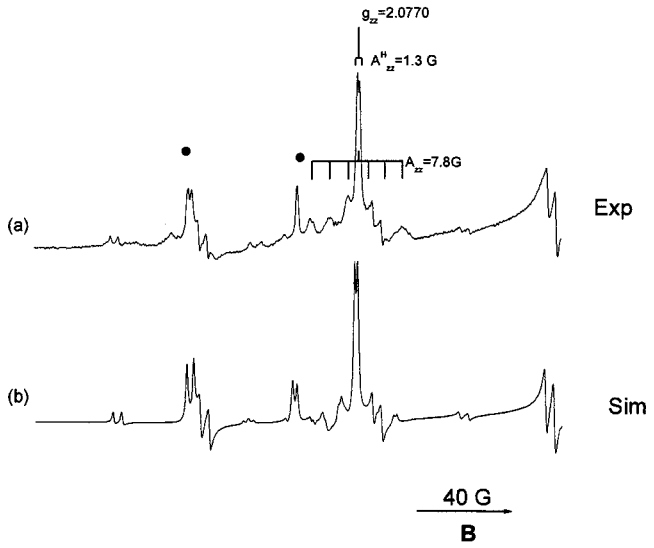

FIG. 5. Expanded part of the g_{zz} region of the 28% ^{17}O enriched O_2^- (Fig. 3). (a) Experimental and (b) computer simulation. The A_{zz}^{O} coupling is illustrated with the stick diagram. The superimposed dominant g_{zz} component due to $^{16}O_2^-$ is also indicated.

V. ANALYSIS OF THE OFF-AXIS EXTRA LINES

As mentioned above, Eq. (2) may sometimes have additional solutions giving rise to extra features in the EPR first derivative powder spectrum. Such off-axis lines were first observed by Neiman and Kivelson in the hyperfine structure of copper phtalocyanine in a H_2SO_4 glass.[22] This problem was theoretically studied by Ovchinnikov and Konstantinov,[27] who derived general conditions for the existence of off-axis extra lines on the basis of a first order treatment which was subsequently refined to include second order terms. From the values of the experimental $\mathbf{A}^{O}$ tensor, and the inequalities given by Eq. (3), it was deduced that five extra absorption lines should be expected in the zx plane, for the investigated superoxide radical. They correspond to $m_1=3$, $\frac{5}{2}$, 2, $\frac{3}{2}$, and 1 transitions reflecting the appearance of additional extrema in a plot of the resonance field $\mathbf{B}_r$ versus θ and ϕ angles. As an illustration, this plot along with the associated topographic map is shown in Figs. 7(a) and 7(b), respectively, for the $m_1=\frac{3}{2}$ transition. Inspection of this figure shows that while the field extrema occur only along the principal directions in the yz and xy planes, for the zx plane there is an additional local minimum at $\theta=28.8°$.

The relation between the $^{17}O_2^-$ EPR spectrum and the angular dependence of the resonance magnetic field in the xz plane for all transitions and both isotopomers is summarized in Fig. 6. The angular dependence of the resonant field was calculated using the second order approximation.[15] The angular dependence of the magnetic field for $(^{17}O–^{17}O)^-$ (solid

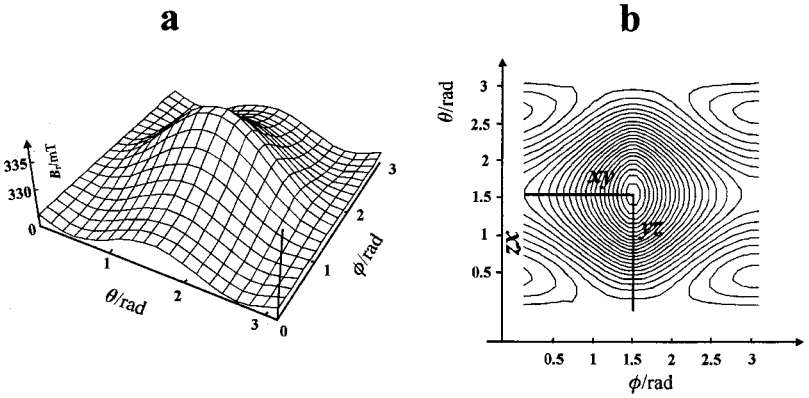

FIG. 7. Resonant field surface $\mathbf{B}_r$ vs θ and ϕ for $m_1 = \frac{3}{2}$ (a), and the corresponding topographic map (b).

lines) shows three additional extrema responsible for the anomalous peaks marked with asterisks, while in the case of the $(^{16}O–^{17}O)^-$ isotopomer (dotted lines) only two such features can be distinguished (the two corresponding lines are marked with dots in Fig. 6). The first peak, related to the transition $\{m_1=3,\ \theta=72.5°\}$, lies very close to the principal one ($\theta=90°$) and is therefore responsible for the anomalous intensity of the combined lines observed in this region of the $(^{17}O–^{17}O)^-$ spectrum. The two other additional extrema for the doubly labeled species are associated with the intermediate transitions $\{m_1=2,\ \theta=38.3°\}$ and $\{m_1=1,\ \theta=22.7°\}$. The extra peaks due to these singularities are intense and well separated from the normal lines.

As mentioned previously the $(^{16}O–^{17}O)^-$ hyperfine structure is complicated by the presence of two extra lines only. The first one is associated with the $\{m_1=\frac{5}{2},\ \theta=51.6°\}$ transition, while the second corresponds to the $\{m_1=\frac{3}{2},\ \theta=28.8°\}$ transition. Similar to the previous case, the $\{m_1=\frac{5}{2},\ \theta=51.6°\}$ line is located close to the normal one $\{m_1=\frac{5}{2},\ \theta=90°\}$ and appears as a shoulder in the spectrum, while the $\{m_1=\frac{3}{2},\ \theta=28.8°\}$ extra line is well separated from the adjacent ordinary peak $\{m_1=\frac{3}{2},\ \theta=90°\}$. This accounts well for the anomalous intensity distribution in this region of the EPR signal. As a result the g_{zz} region contains nine intense peaks (i.e., four ''normal'' lines at $\theta=90°$, and five extra lines) which are superimposed on a weaker and less resolved A_{zz} pattern, in accordance with the experimental observation.

Since the hyperfine structure along the z direction is weak and occurs in the most congested part of the spectrum, the dominant extra lines were used as a reference to pin down the precise value of A_{zz}. Following the second order treatment, the positions of the overshoots in the zx plane are related to the A_{zz} value according to the following equation:[22]

$$B_{zx}(m_I)=h\nu/\beta g_{zx}\{1-m_I K_{zx}-[I(I+1)-m_I^2](A'^2_{yy}+A'^2_{zz}A'^2_{xx}/K^2_{zx})/4-m_I^2(K^2_{zx}-A'^2_{zz})(A'^2_{xx}-K^2_{zx})/2K^2_{zx}\}, \quad (5)$$

where $A'_{ij}=A_{ij}/h\nu$. The g_{zx} value corresponding to the extra absorption peak may be calculated from

$$g_{zx}=g^2_{zz}g^2_{xx}(A'^2_{zz}-A'^2_{xx})/(g^2_{zz}-g^2_{xx})(\Delta_{zx}-K^2_{zx}), \quad (6)$$

where Δ_{zx} is defined as

$$\Delta_{zx}=(g^2_{zz}A'^2_{zz}-g^2_{xx}A'^2_{xx})/(g^2_{zz}-g^2_{xx}). \quad (7)$$

The calculation of K_{ij} is more complex, and has been determined to first order only:

$$K^{(0)}_{zx}=(1/4m_I)[1-(1+m_I^2\Delta_{zx})^{1/2}]. \quad (8)$$

On the basis of the previous set of equations, the $B_{zx}(m_I)$ positions of the five overshoot peaks have been reproduced within a precision of 2–3 G using $A_{zz}=8\pm2$ G. This latter value was next used as a starting point for the complete simulation of the spectrum. The close similarity between the experimental and simulated spectra for the superoxide species (Fig. 5) adds further reliability to the data and approach adopted in this work for an accurate and reliable determination of the ^{17}O hyperfine tensor.

VI. DISCUSSION

A. The g tensor

Analysis of the **g** tensor for surface adsorbed superoxide species was usually performed in the past (Ref. 3 and references therein) approximating to first order the set of equations rigorously derived by Kanzig and Cohen in the case of O_2^- trapped in a single crystal of potassium chloride.[28] This crude approximation was, however, adequate to the relatively low resolution of most surface O_2^- powder spectra.

In the present case the excellent quality of the spectra prompted us to go back to the original analysis of Kanzig and Cohen[28] as follows. The **g** tensor of the trapped superoxide species is in agreement with that expected for a bound $^2\Pi_{3/2}$ state characterized by the unpaired electron on the $2p\pi_g^x$ antibonding orbital. The spin orbit coupling along with the C_{2v} crystal field produces to an orthorhombic **g** tensor[28] given by

$$g_{xx}=2.0023[\Delta^2/(\lambda^2+\Delta^2)]^{1/2}-\lambda/E\{1-[\lambda^2/(\lambda^2+\Delta^2)]^{1/2}-[\Delta^2/(\lambda^2+\Delta^2)]^{1/2}\},$$

$$g_{yy}=2.0023[\Delta^2/(\lambda^2+\Delta^2)]^{1/2}-\lambda/E\{[\lambda^2/(\lambda^2+\Delta^2)]^{1/2}-[\Delta^2/(\lambda^2+\Delta^2)]^{1/2}-1\}, \quad (9)$$

$$g_{zz}=2.0023+2[\lambda^2/(\lambda^2+\Delta^2)]^{1/2},$$

TABLE II. Molecular parameters derived from the g tensor, and spin densities obtained from the $\mathbf{A}^{O}$ tensor.

Species	λ (eV)	Δ (eV)	E (eV)	ρ_{π}^{x}	ρ_{π}^{y}	ρ_{s}
$\eta^2O_2^-$/MgO	0.0115	0.3067	3.04	0.495	−0.024	0.011

where λ is the spin-orbit coupling constant, Δ is the $2p\pi_g^x - 2p\pi_g^y$ separation and E is the $2p\pi_g^x - 2p\sigma_g$ separation. It follows then that $g_{zz} \gg g_{yy} > g_{xx}$, as experimentally observed. The λ, Δ, and E parameters were calculated by least squares fitting of the experimental **g** tensor to these equations. The results of the optimization are summarized in Table II. The λ value is smaller in comparison to the estimated atomic one ($\lambda_0 = 0.014$ eV)[29] and we assign this deviation to quenching of the angular momentum l about the internuclear axis caused by the crystal field ($l < 1$). The results indicate that the SOMO is confined essentially to the $2p\pi_g^x$ orbital with a small contribution from the $2p\pi_g^y$ and $2p\sigma$ orbitals.

B. The A tensor

As mentioned in the Introduction the first analysis of the hyperfine structure of O_2^- on MgO[5] done in the late 1960s was deeply affected by the lack of information on two (A_{yy} and A_{zz}) of the three components of the experimental **A** tensor.

Once again, the nice resolution of the spectra here reported for CVD MgO and the results of the complex simulation of the whole line pattern allows us a thorough and conclusive analysis of the spin population of the surface adsorbed species.

Based on the preceding discussions for the ^{17}O hyperfine interaction (Sec. IV), the sign of the A_{xx} component has been taken as negative, in agreement with results reported by other authors.[3] The $^{17}O_2^-$ tensor deduced from the current spectra is therefore

$$A^{O}/\beta_e g = \begin{vmatrix} -76 & & \\ & +7.8 & \\ & & +7.3 \end{vmatrix} \text{G}$$

or

$$A^{O}/h = \begin{vmatrix} -212.9 & & \\ & +21.9 & \\ & & +21.2 \end{vmatrix} \text{MHz}.$$

This result represents the first complete experimental determination of the $^{17}O_2^-$ hyperfine tensor for the adsorbed superoxide species.

The localized spin model, successfully applied by Lindsay *et al.*[30] for analysis of the O_2^- EPR spectrum, can be used to rationalize the observed ^{17}O tensor. In this model, a quarter ($\rho/4$) of the electron spin density is assumed to be concentrated equally in each of the four lobes of the oxygen $2p_{\pi}^x$ orbitals at an effective distance R_p from the nucleus (Fig. 1). The magnetic interactions within the superoxide radical are indicated in the figure with the dotted arrows. The spin density on the $2p_{\pi}^x$ orbital gives rise to a certain degree of spin polarization of the inner s-orbital for each ^{17}O atom as well as to polarization of the σ-bond connecting both oxygen nuclei. However, in the latter case the spin density induced by one atom is counterbalanced by an equivalent amount of opposite spin density generated by interaction with the second atom, since both nuclei are magnetically equivalent. Therefore the resultant polarization can be accounted for by a simple McConnel-type equation.

The localized spin model implies two types of dipolar interactions: (i) *a through bond* intraatomic interaction on the coupling atom gauged by the tensor $\mathbf{T}^{O} = g_e\beta_e g_O \beta_n 1/\langle r^3 \rangle \times [\frac{4}{5}, -\frac{2}{5}, -\frac{2}{5}]$ and (ii) *a through space* inter-atomic coupling $\mathbf{A}_d$ between the ^{17}O nucleus and the spin density on the adjacent oxygen. As a result the $\mathbf{A}^{O}$ tensor is comprised of the following three terms:

$$\mathbf{A}^{O} = \langle a^{O} \rangle + \mathbf{T}^{O} + \mathbf{A}_d \tag{10}$$

with $\langle a^{O} \rangle = a_{\text{iso}} + P\langle g \rangle$, where a_{iso} is the isotropic Fermi contact interaction and $P\langle g \rangle$ is the pseudocontact term.

The traceless tensor $\mathbf{A}_d$ can be approximated by the proximal dipole formula originally proposed by Gordy for organic π radicals:[31]

$$\begin{aligned} A_{xx}/h &= -14.1\rho_{\pi}^{O} g_O (2R_p^2 - R_{OO}^2)/(R_{OO}^2 + R_p^2)^{5/2}, \\ A_{yy}/h &= -14.1\rho_{\pi}^{O} g_O /(R_{OO}^2 + R_p^2)^{3/2}, \\ A_{zz}/h &= 14.1\rho_{\pi}^{O} g_O (2R_{OO}^2 - R_p^2)/(R_{OO}^2 + R_p^2)^{5/2}. \end{aligned} \tag{11}$$

The R_p value has been estimated from the known atomic value of $\langle r^{-3} \rangle$ for oxygen using the expression $R_p = \langle r \rangle = 1.75\langle r^{-3} \rangle^{-1/3} = 0.54$ Å proposed elsewhere by Lindsay.[30] The internuclear distance $R_{OO} = 1.35$ Å was derived from quantum chemical calculations of O_2^- on MgO.[32] Upon substitution of the numerical values into this equation we obtain $A_d/h = |1.02, 1.74, -2.76| \times$ MHz ($A_d/\beta_e g = |0.36, 0.62, -0.94| \times$ G). Thus the corrected $A^{O}/\beta_e g$ tensor assumes the form:

$$\begin{vmatrix} -76.36 & & \\ & +7.18 & \\ & & +8.24 \end{vmatrix} = -20.3 + \begin{vmatrix} -56 & & \\ & +27.5 & \\ & & +28.6 \end{vmatrix}.$$

These results can be compared with those recently calculated by Soave *et al.*[32] for O_2^- on MgO (Table I). The dipolar tensor is in excellent agreement with our experimental data. The a_{iso} term, which is more difficult to theoretically predict with high accuracy, is apparently underestimated in the calculations, although the discrepancy is not dramatic considering that it corresponds to an absolute difference of 0.006 in the total spin density on the $2s$ orbital.

C. Spin density on the superoxide ion

To thoroughly analyze the spin density associated to the various oxygen orbitals, the $\mathbf{A}^{O}/h$ matrix can be decomposed as follows:

$$\begin{vmatrix} -213.93 & & \\ & +20.19 & \\ & & 23.98 \end{vmatrix} = -60.7 + \begin{vmatrix} -149.8 & & \\ & +74.9 & \\ & & 74.9 \end{vmatrix} + \begin{vmatrix} -3.5 & & \\ & 7.07 & \\ & & -3.5 \end{vmatrix} + \begin{vmatrix} 0.12 & & \\ & -1.07 & \\ & & 13.33 \end{vmatrix},$$

where the first and second matrices are related to the decomposition along the *x* and *y* axis, respectively, while the third one is a correction which accounts for the **L·I** coupling between the nuclear and orbital magnetic moments calculated from the Weltner's formula.[18] Because of the pronounced derivation of g_{zz} from 2.0023 and the small value of A_{zz}, the correction is sensible for this particular component.

The experimental value for $a_{iso}=-60.7$ (-21.3 G) is in line with that predicted by applying a simple equation proposed by Melamud and Silver for organic and inorganic oxygen containing π radicals.[33] This equation can be written as $a_{iso}=Q^O\rho_\pi^O$, where $Q^O=41\pm3$ G and ρ_π^O is the spin density on the $2p_\pi^x$ orbital. For an oxygen radical with magnetically equivalent nuclei and a unit π spin density (*vide infra*) the value of $a_{iso}=(41\pm3)/2=20.5\pm1.5$ G is expected, if the spin polarization only is involved. This value compares very well with the observed one, indicating a true π character of the investigated superoxide radical.

The dipolar tensor components *B* along the *x* and *y* directions indicate that the spin densities are positive in the $2p_\pi^x$ orbital but negative in the $2p_\pi^y$ orbital, in line with previous observations for superoxide species bound to Co^{2+} ions.[21] Using the reported atomic value for the dipolar ^{17}O hyperfine constant, $B_o=4/5g_O\beta_n\langle r^{-3}\rangle_{2p}=-336.8$ MHz, we can assess the spin density on the oxygen $2p\pi_g$ orbitals, by comparing the experimentally derived dipolar component *B* with that value, using the classic formula $\rho_\pi^i=B_i/B_o$. In our case the following values of $\rho_\pi^x=B_x/B_o=-149.8/-336.8=0.44$ and $\rho_\pi^y=B_y/B_o=7.07/-168.4=-0.021$ were calculated. However, through an increased nuclear screening, the resultant negative charge on the ^{17}O atom of the superoxide radical will decrease the anisotropic coupling constant over that expected for the neutral species, and the spin densities calculated above must therefore be further corrected. The relevant semi-empirical corrections were proposed by Townes and Schawlow.[34] For a net negative charge c^- on the atom the formula for the spin density takes the form

$$\rho_\pi=B(1+c^-\epsilon)/B_o, \tag{12}$$

where ϵ is the charge-correction constant tabulated elsewhere.[34] Taking $c^-=0.5$ and $\epsilon=0.25$, the values of $\rho_\pi^x=0.495$ and $\rho_\pi^y=-0.024$ were obtained after substitution of the remaining numerical values into this equation (Table II). The net spin density on the $2s$ orbital (ρ_s) was calculated using $a_{iso}=\rho_s A_0$, which gives $\rho_s=-60.7/-5263=0.011$ for $A_0=-5263$ MHz.

The total spin density on the redox $2p\pi_g^x$ molecular orbital is equal to 0.99. This result indicates that within the limits of the approximation adopted the electron transfer from the surface $F_S^+(H)$ center towards the adsorbed dioxygen molecule is practically complete.

VII. CONCLUSIONS

The resolution of the EPR spectrum due to the $^{17}O_2^-$ radical trapped on the MgO surface is significantly improved by (i) use of a highly crystalline high surface area material, (ii) adopting a particular adsorption procedure which prevents superoxide speciation, and (iii) control of the isotopomer composition with two selected ^{17}O enrichments. The spectral pattern is complicated by the simultaneous presence of a high number of ''normal'' hyperfine lines and also by several off-axis extra features, which have prohibited the accurate interpretation of the A_{yy} and A_{zz} components in the past. The ^1H superhyperfine structure, from the $O_2^-\cdots OH$ interaction, along with the positions of the extra absorption lines have been used as auxiliary source of information to determine the complete ^{17}O hyperfine tensor. The composition of this tensor was analyzed in detail using a localized spin model. The evaluated spin density distribution within the superoxide radical is consistent with a complete electron transfer from a surface $F_S^+(H)$ donor center to the dioxygen acceptor counter part, in agreement with recent *ab initio* theoretical calculations.[32]

ACKNOWLEDGMENTS

This work was supported in part by the Italian INFM, through the PRA-ISADORA project. The authors wish to thank Dr. Frank Mabbs and Dr. David Collision (Manchester University, UK) for allowing us use of their computer simulation program and Dr. Robert Farley (Cardiff University, UK) for technical assistance in the analysis of the off-axis extra features. Funding from the ESPRC for the National EPR Service is also gratefully acknowledged. Z.S. is grateful to the Jagiellonian University for the A. Krzyżanowski stipend.

[1] Z. Sojka, Catal. Rev. - Sci. Eng. **37**, 461 (1995).
[2] M. Che and A. J. Tench, Adv. Catal. **31**, 77 (1982).
[3] M. Che and A. J. Tench, Adv. Catal. **32**, 1 (1983).
[4] M. Anpo, M. Che, B. Fubini, E. Garrone, E. Giamello, and M. C. Paganini, Top. Catal. **8**, 189 (1999).
[5] A. J. Tench and P. Holroyd, Chem. Commun. (London) **1968**, 471.
[6] E. Giamello, D. Murphy, L. Ravera, S. Coluccia, and A. Zecchina, J. Chem. Soc., Faraday Trans. **90**, 3167 (1994).
[7] D. Murphy and E. Giamello, J. Phys. Chem. **99**, 15172 (1995).
[8] E. Giamello, M. C. Paganini, D. Murphy, A. M. Ferrari, and G. Pacchioni, J. Phys. Chem. B **101**, 971 (1997).
[9] M. Chiesa, M. C. Paganini, E. Giamello, and D. M. Murphy, Langmuir **13**, 5306 (1997).
[10] M. C. Paganini, M. Chiesa, E. Giamello, G. M. Martra, S. Coluccia, and D. M. Murphy, Surf. Sci. **421**, 240 (1999).
[11] D. Murphy, R. D. Farley, I. J. Purnell, C. C. Rowlands, A. R. Yacob, M. C. Paganini, and E. Giamello, J. Phys. Chem. **103**, 1944 (1999).
[12] E. Giamello, M. C. Paganini, M. Chiesa, D. M. Murphy, R. Soave, G. Pacchioni, and A. Rockenbauer, J. Phys. Chem. B **104**, 1887 (2000).
[13] M. Chiesa, E. Giamello, M. C. Paganini, G. Pacchioni, R. Soave, D. M. Murphy, and Z. Sojka, J. Phys. Chem. B **105**, 497 (2001).

[14] E. Knözinger, K.-H. Jacob, S. Singh, and P. Hofmann, Surf. Sci. **290**, 388 (1993).
[15] F. E. Mabbs and D. Collison, in *Electron Paramagnetic Resonance of d-Transition Metal Compounds* (Elsevier, Amsterdam, 1992).
[16] E. Giamello, D. M. Murphy, E. Garrone, and A. Zecchina, Spectrochim. Acta, Part A **49**, 1323 (1993).
[17] M. Che, E. Giamello, and A. J. Tench, Colloids Surf. **13**, 231 (1985).
[18] W. Weltner, Jr., in *Magnetic Atoms and Molecules* (Dover, New York, 1983).
[19] N.-B. Wong and J. H. Lunsford, J. Chem. Phys. **55**, 3007 (1971).
[20] J. A. De Gray and P. H. Rieger, Bull. Magn. Reson. **8**, 95 (1987).
[21] L. C. Dickinson and J. C. W. Chien, Proc. Natl. Acad. Sci. U.S.A. **77**, 1235 (1980).
[22] R. Neiman and D. Kivelson, J. Chem. Phys. **36**, 156 (1961).
[23] G. Pacchioni, A. M. Ferrari, and E. Giamello, Chem. Phys. Lett. **255**, 58 (1996).
[24] E. Giamello, E. Garrone, P. Ugliengo, M. Che, and A. J. Tench, J. Chem. Soc., Faraday Trans. 1 **85**, 3987 (1989).
[25] Z. Sojka, M. Chiesa, E. Giamello, and M. C. Paganini, Stud. Surf. Sci. Catal. **140**, 443 (2001).
[26] T. Ito, T. Watanabe, T. Tashiro, and K. Toi, J. Chem. Soc., Faraday Trans. 1 **85**, 2381 (1989).
[27] V. Ovchinnikov and V. N. Konstantinov, J. Magn. Reson. (1969-1992) **32**, 179 (1979).
[28] W. Kanzig and M. H. Cohen, Phys. Rev. Lett. **3**, 509 (1959).
[29] P. Kasai, J. Chem. Phys. **43**, 3322 (1965).
[30] D. M. Lindsay, D. R. Herschbach, and A. L. Kwiram, Chem. Phys. Lett. **25**, 175 (1974).
[31] W. Gordy, in *Theory and Applications of Electron Spin Resonance*, edited by W. West (Wiley, New York, 1980).
[32] R. Soave, A. M. Ferrari, and G. Pacchioni, J. Phys. Chem. B **105**, 9798 (2001).
[33] E. Melamud and B. L. Silver, J. Phys. Chem. **77**, 1896 (1973).
[34] C. H. Townes and A. L. Schawlow, in *Microwave Spectroscopy* (Dover, New York, 1975).